International Journal of Nanomedicine

Dovepress
open access to scientific and medical research

Open Access Full Text Article

ORIGINAL RESEARCH

Fluorescence properties of curcumin-loaded nanoparticles for cell tracking

This article was published in the following Dove Press journal:
International Journal of Nanomedicine

Bassam Felipe Mogharbel,[1] Julio Cesar Francisco,[1] Ana Carolina Irioda,[1] Dilcele Silva Moreira Dziedzic,[1] Priscila Elias Ferreira,[1] Daiany de Souza,[1] Carolina Maria Costa Oliveira de Souza,[1] Nelson Bergonse Neto,[2] Luiz Cesar Guarita-Souza,[2] Celia Regina Cavichiolo Franco,[3] Celso Vataru Nakamura,[4] Vanessa Kaplum,[4] Letícia Mazzarino,[5] Elenara Lemos-Senna,[6] Redouane Borsali,[7] Paula A Soto,[8] Patricia Setton-Avruj,[8] Eltyeb Abdelwahid,[9] Katherine Athayde Teixeira de Carvalho[1]

[1]Cell Therapy and Biotechnology in Regenerative Medicine Department, Pelé Pequeno Príncipe Institute, Child and Adolescent Health Research and Pequeno Príncipe Faculty, Curitiba, Paraná, Brazil; [2]Institute of Biological and Health Sciences, Pontifical Catholic University of Paraná (PUCPR), Centro de Ciências Biológicas e da Saúde (CCBS), Curitiba, Brazil; [3]Cell Biology Department, Federal University of Paraná, Curitiba, Paraná, Brazil; [4]Department of Pharmaceutical Sciences, Universidade Estadual de Maringá, Maringá, Paraná, Brazil; [5]Department of Pharmaceutical Sciences, NanoBioMat Laboratory, Federal University of Santa Catarina, Florianópolis, Santa Catarina, Brazil; [6]Department of Pharmaceutical Sciences, Federal University of Santa Catarina, Florianópolis, Santa Catarina, Brazil; [7]Centre de Recherches sur les Macromolécules Végétales (CERMAV), Centre National de la Recherche Scientifique (CNRS), University Grenoble Alpes, F-38000, Grenoble, France; [8]Instituto de Química y Físicoquímica Biológica (IQUIFIB), Departament of Química Biológica, Facultad de Farmacia y Bioquímica, Universidad de Buenos Aires (UBA) Consejo nacional de Investigaciones Científicas y Técnicas (CONICET), Buenos Aires, Argentine; [9]Feinberg School of Medicine, Feinberg Cardiovascular Research Institute, Northwestern University, Chicago, Il, USA

Correspondence: Katherine Athayde Teixeira de Carvalho
Cell Therapy and Biotechnology in Regenerative Medicine Department, Pelé Pequeno Príncipe Institute, Child and Adolescent Health Research and Pequeno Príncipe Faculty, Ave. Silva Jardim. 1632, BOX 80.240-020, Curitiba, Paraná, Brazil
Tel +55 413 310 1719
Email katherinecarv@gmail.com

Background: Posttransplant cell tracking, via stem cell labeling, is a crucial strategy for monitoring and maximizing benefits of cell-based therapies. The structures and functionalities of polysaccharides, proteins, and lipids allow their utilization in nanotechnology systems.

Materials and methods: In the present study, we analyzed the potential benefit of curcumin-loaded nanoparticles (NPC) using Vero cells (in vitro) and NPC-labeled adipose-derived mesenchymal stem cells (NPC-ADMSCs) (in vivo) in myocardial infarction and sciatic nerve crush preclinical models. Thereafter, transplantation, histological examination, real time imaging, and assessment of tissue regeneration were done.

Results: Transplanted NPC-ADMSCs were clearly identified and revealed potential benefit when used in cell tracking.

Conclusion: This approach may have broad applications in modeling labeled transplanted cells and in developing improved stem cell therapeutic strategies.

Keywords: mesenchymal stem cells, transplantation, cell marking, myocardium infarction, sciatic nerve crush

Introduction

Regenerative medicine has the objective to restore the lost functions of an organ or tissue[1] and has been searching for newer alternatives for posttransplant cell tracking in cell-based therapies. Thus, stem cell labeling is a crucial aim in research, since the techniques that are usually used are invasive or contrast dependent.[2] Materials used for this purpose include quantum dots, carbon nanotubes, and nanoparticles containing both inorganic elements such as iron, silver, copper, and zinc oxide and synthetic or biological elements. Markers in this context vary in size, material, antigenicity, and degradability, although all of them need to ensure tolerance and avoid side effects.[3–6]

In such scenario, biopolymers emerge as a promising technique. The structures and functional properties of polysaccharides, proteins, and lipids allow their utilization in nanotechnology systems.[7,8] In particular, curcumin properties and its fluorescence have been widely described in the literature.[9–11]

Curcumin has been used in several studies and shown therapeutic promises, particularly its anti-oxidant and anti-cancer properties.[12,13] In addition, curcumin can enhance adipose-derived mesenchymal stem cell (ADMSC) survival after transplantations, mostly through heme oxygenase-1 expression, which prevents cell death caused by oxidative stress.[14,15] Interestingly, ADMSC pretreated with curcumin displayed improved myocardial recovery through an increase in vascular endothelial growth factor production, enhanced antiapoptotic ability, stimulation of neovascularization in peri-infarcted area, and reduced infarct size.[16] However, its fluorescence properties as an imaging probe are not utilized as described in this study.

submit your manuscript | www.dovepress.com
Dovepress
http://dx.doi.org/10.2147/IJN.S171099

On the other hand, extensive clinical trials using stem cells, particularly in the treatment of onco-hematological diseases, opened up the possibility of evaluating stem cells for treatment of non-hematopoetic affections. Mesenchymal stem cells (MSCs) represent a promising source for regeneration and repair of various tissues, due to their presence in adult solid organs as well as in the mesoderm of embryonic tissue.[17,18] In this study, we investigated the fluorescence properties of curcumin-loaded nanoparticles for tracking cellular therapy.

Materials and methods

The experimental design is presented in Figure 1.

In vitro studies

Preparation and characterization of nanoparticles

Unloaded polycaprolactone nanoparticles (NP) and curcumin-loaded polycaprolactone nanoparticles (NPC) were prepared using the nanoprecipitation method as previously described by Mazzarino et al.[19] Particle size and zeta potential were detected by dynamic light scattering (DLS) and laser-doppler anemometry, respectively, using a Zetasizer Nano Series (Malvern Instruments, Worcestershire, UK). Curcumin was determined using a UV/Vis spectrophotometric method.[20] The total concentration of curcumin in the nanoparticle suspensions was measured after their complete dissolution in acetonitrile. Encapsulation efficiency was calculated by the difference between the total concentration of curcumin found in the nanoparticle suspensions and the concentration of the free drug in the ultrafiltrate obtained after the separation of nanoparticles by ultrafiltration/centrifugation.

Nanoparticle flow cytometric analysis

Flow cytometric analysis using 488 nm blue laser was made to confirm the emission wavelength of the NPC using the cytometer FACS Canto II (Becton Dickinson Biosciences,

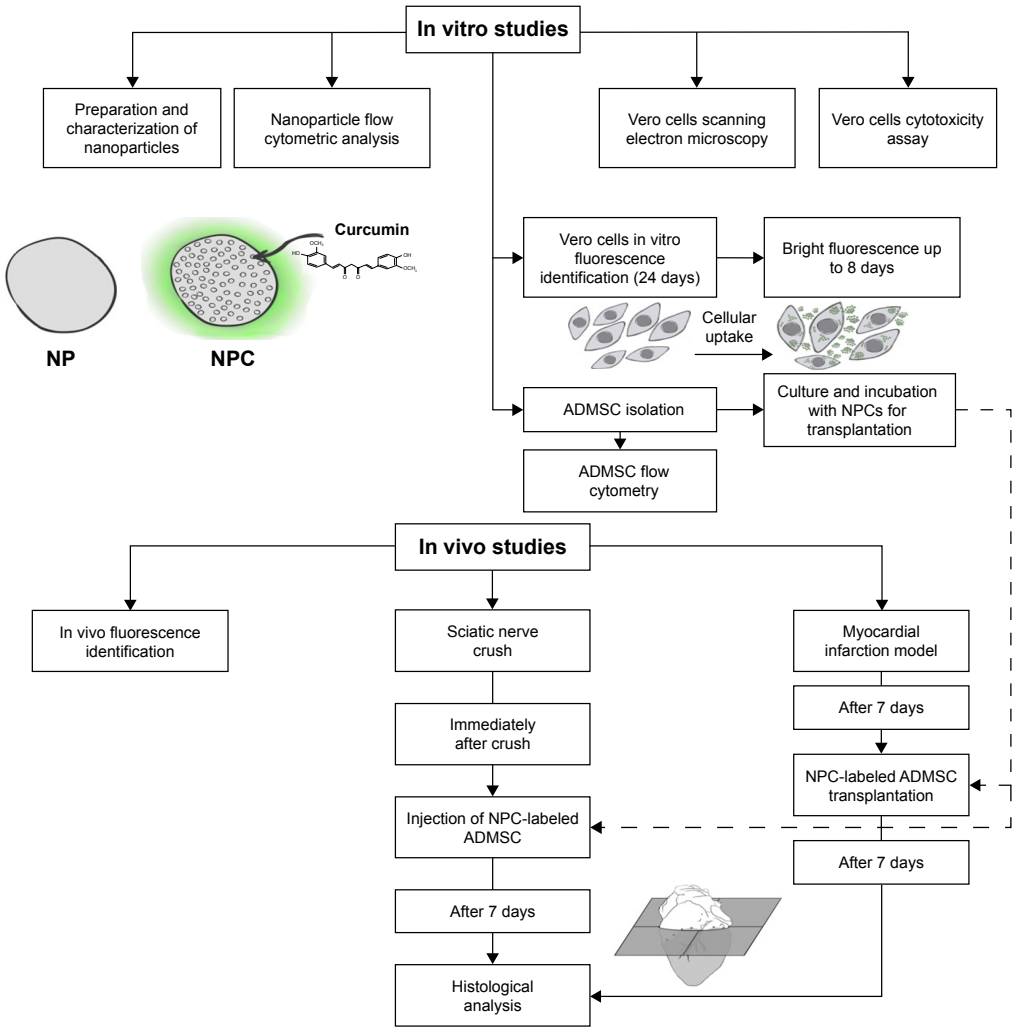

Figure 1 Diagram for in vitro and in vivo studies.
Abbreviations: NP, unloaded polycaprolactone nanoparticles; NPC, curcumin-loaded polycaprolactone nanoparticles; ADMSC, adipose-derived mesenchymal stem cells.

Franklin Lakes, NJ, USA). The NPCs were suspended in PBS (Sigma-Aldrich Co., St Louis, MO, USA) to obtain a final concentration of 10 µM and 1 mL of volume. In addition, a 1 mL suspension of NP was prepared. The data were analyzed with Infinicyt software (Cytognos S.L., Santa Marta de Tormes, Salamanca, Spain).

Scanning electronic microscopy

The used Vero cells (CCL-81, TECPAR) were approved by institutional committee for laboratory animal control, number: 025–12 01 2014 of CEUA-Complexo Hospitalar Pequeno Príncipe (Curitiba, Brazil). Vero cells were seeded in wells with cover slips until reaching 80% of confluence. At this point, the culture medium was replaced with a fresh culture medium containing 30 µM NPC. The wells were washed with 0.1M sodium cacodylate buffer, pH 7.4 at 4°C. The cells were then fixed in Karnovski solution (2% gluteraldehyde, 4% paraformaldehyde, 1 mM calcium chloride [$CaCl_2$] in 0.1M cacodylate buffer, pH 7.2–7.4) for an hour, and then washed three times in 0.1M sodium cacodylate buffer, pH 7.4. Then the cells were dehydrated with crescent ethanol concentrations (30%, 50%, 70%, 90%, and 100% twice) for 10 minutes at each concentration. Afterward, the critical point and gold coating were obtained using the equipment (CPD-Balzers Union/Baltec, Germany) for (CPD 030 BALTEC, Pfäffikon, Switzerland). The cells were then analyzed with scanning electron microscopy (SEM) (Vega-3LMU; Tescan, Brno, Kahoutovice-Czec Republic).

Cytotoxicity

The cytotoxicity was evaluated by using the MTT assay. These NPC were cultured in DMEM-High Glucose (Sigma-Aldrich Co.) containing 10% fetal bovine serum (Thermo Fisher Scientific, Waltham, MA, USA), 1% penicillin (100 U/mL) and streptomycin (100 µg/mL) (Thermo Fisher Scientific) and incubated at 37°C and 5% CO_2. For the MTT assay, cells were seeded in a 24-well plate (1×10^4 cells/cm^2) in media containing 30 µM concentration of NPC and incubated at 37°C for 24 hours. After incubation, the cells were washed with PBS, the medium was changed, and MTT solution (Sigma-Aldrich Co.) was added and incubated for 3 hours at 37°C. Subsequently, cells were washed to remove the supernatant, and 100 µL of dimethyl sulfoxide (Sigma-Aldrich Co.) was added. The cells were then shaken for 5 minutes, and the absorbance was measured at 595 nm on a microplate reader (EL800; Biotek Instruments Inc., Winooski, VT, USA).

Statistical analysis was done by using the one-way ANOVA test. *P*-values <0.05 were considered to be significant and calculated using the Graph-Pad Prism (GraphPad Software Inc., La Jolla, CA, USA) software. The graph shows 95% CI of the mean ± SD.

In vitro fluorescence identification

Vero cells were seeded on 96-well plates (1×10^4 cells/cm^2) and treated with 30 µM NPC for 72 hours at 37°C. After incubation, cells were washed with PBS and new culture medium was added. The cells were evaluated for 24 days, with medium changed every 2 days. Images were captured using a fluorescence microscope (Axio Vert.A1; Carl Zeiss Meditec AG, Jena, Germany).

ADMSC isolation, culture, and incubation with NPCs for transplantation

The cells were isolated from inguinal fat of Wistar rats by enzymatic dissociation with the aid of Collagenase IA (Sigma-Aldrich Co.). Cells were cultured in DMEM F12 (Sigma-Aldrich Co.) containing 10% fetal bovine serum (Thermo Fisher Scientific), penicillin (100 U/mL), and streptomycin (100 µg/mL) (Sigma-Aldrich Co.) at 37°C and 5% CO_2. Cells were then seeded in 24-well plates (1×10^5 cells/cm^2) and incubated for 72 hours with NPC at 37°C. After incubation, cells were washed with PBS for supernatant removal. Images were captured using a fluorescence microscope to demonstrate the fluorescence of NPCs in cultured ADMSC.

On the other hand, and following incubation with NPC, another group of cells was washed with PBS and treated with 100 µL of trypsin (Thermo Fisher Scientific) for 5 minutes at 37°C. Cells were then added to culture medium containing fetal bovine serum to stop trypsin action and were subjected to centrifugation for 5 minutes at 1,400 rpm. The supernatant was discarded and the cells were suspended in 25 µL of culture medium for transplantation.

Cell flow cytometric analysis

The immunophenotyping of the cells was done with the flow cytometric apparatus FACS Canto II (Becton Dickinson Biosciences) and using cell membrane markers: CD34 (phycoerythrin [PE]), CD45 (PerCP-Cy5-5), CD73 (fluroscein isothiocyanate [FITC]), and CD90 (PE-CY7) (Becton Dickinson Bioscience). The following isotype negative controls were used: FITC Mouse IgG1 κ, PE Mouse IgG2a κ, PE-Cy7 Mouse IgG1 κ, PERCP Mouse IgG1 κ (Becton Dickinson Bioscience).

A fraction of the cells were transferred to two cytometry tubes containing 100 µL of PBS and incubated for 15 minutes in a dark room with the cell membrane markers as well as with the isotype controls. After incubation, the tubes were

washed with PBS and then centrifuged for 5 minutes at 1,400 rpm. The cells were suspended with PBS and analyzed by the flow cytometer.

In vivo studies

All rats were kept under standard conditions with food and water ad libitum on a 12-hour day/night cycle (light on at 7:00 am). All animals were euthanized with a lethal dose of pentobarbital sodium (thiopental) 200–250 mg/kg intraperitoneally (IP).

The protocol of myocardial and in vivo analysis studies was approved by each institutional committee for laboratory animal control (number: 025–12 01 2014 of CEUA – Complexo Hospitalar Pequeno Príncipe [Curitiba, Brazil]) and for crush studies (number: 0040963/2015 of CUDAP: EXP-UBA, Facultad de Farmacia y Bioquímica Universidade de Buenos Aires [Buenos Aires, Argentina]) in accordance with the guidelines for the care and use of laboratory animals published by ARRIVE and the US National Institutes of Health.[21]

In vivo fluorescence identification

Anesthetized animals were placed in the Carestream in vivo MS FX-Pro (Bruker Corporation, Billerica, MA, USA) for quantification of the baseline. Then the abdominal region was divided in four quadrants and each one was injected with 200 µL of a different solution. The four solutions injected were NP-ADMSC, NPC-ADMSC, NP, and NPC. The region of interest was excited at 480 nm and the emission wavelength was 535 nm.

Fluorescence and histological analysis

NPC-labeled ADMSC were subcutaneously injected in Wistar rats subjected to different experimental conditions and then analyzed for fluorescence detection and histological studies.

Myocardial infarction model

Adult male Wistar rats (70 days old, 270–300 g body weight) (n=4) were anesthetized with ketamine (75 mg/kg IP) and xylazine (10 mg/kg IP). Each animal was submitted to a trichotomy on the left ventrolateral portion of the chest, immediately before the surgical procedure. The animal was positioned in supine with a slight tilt to the right, thus facilitating the exposure of the area to be approached. Rats were then subjected to orotracheal intubation and left thoracotomy in the third intercostal space, following antisepsis in chest. After opening the left pleura, the pericardium was exposed and the heart visualized. Subsequently, the left coronary artery was ligated with polypropylene nonabsorbable monofilament suture 4.0. The infarcted area was immediately identified by heart color changes. Afterward, the heart was replaced in the chest; the hyperinflated lungs and the chest wall were sutured layer by layer using mononylon sutures (nonabsorbable 3.0). After recovery from anesthesia, the animals were kept in cages with water and food ad libtum (Figure S1).

ADMSC labeled with NPC transplantation in myocardial infarction

One week after surgeries, the animals were anesthetized, left lateral thoracotomy was performed, and the heart was exposed, prepared, and analyzed.

The NPC-labeled ADMSC were injected into the transition area of the posterior wall of the left ventricle, and the infusion of 25 µL of cell solution was done at a concentration of 5×10^5 cells/mL using Hamilton syringe (702RN; Hamilton Company, Reno, NV, USA) (Figure S2).

Histological analysis

The euthanasia was done at 1 week after transplantation of MSC containing the NPC, and the hearts were collected for histological analysis. The hearts were immediately frozen in liquid nitrogen and the sections (8–10 µm thick) were obtained using a cryostat microtome (Leica Biosystems Nussloch GmbH, Nussloch, Germany) at –20°C.

Some of the sections were stained with H&E to evaluate myocardial morphology and the cross-sections allowed us to evaluate all heart layers, including the infarcted region, where NPC-labeled ADMSC would be found; other sections were incubated at room temperature with Hoechst 33258 (Thermo Fisher Scientific) for the nuclei stain (0.2 µg/mL), and images were captured using a fluorescence microscope (Axio Vert.A1; Carls Zeiss).

Sciatic nerve crush

Male and female Wistar rats (70 days old, 270–300 g body weight) were anesthetized with ketamine (75 mg/kg IP) and xylazine (10 mg/kg IP). Their right sciatic nerves were then exposed at mid-thigh level by dissecting an 8–10 mm long segment from the surrounding tissue and crushed for 8 seconds with jeweler's forceps (N°5 Dumont forceps) as previously described.[22] After 7 days, both sciatic nerves were carefully dissected out; the proximal, crush, and distal areas in the right nerve (ipsilateral) and the left nerve (contralateral) were identified.

Table 1 Physicochemical properties of unloaded (NP) and curcumin-loaded (NPC) nanoparticles

Variable	NP	NPC
Particle size (nm)	194.9	189.4
Polydispersity index	0.082	0.095
Zeta potential (mV)	0.092	–0.112
Curcumin content (μg/mL)	–	426.0
Encapsulation efficiency (%)	–	99.8

Abbreviations: NP, unloaded polycaprolactone nanoparticles; NPC, curcumin-loaded polycaprolactone nanoparticles.

Injection of isolated ADMSC

ADMSCs were isolated from two male rats. Immediately after crush, an intravascular injection of 200 μL of media containing 3×10^6 NPC-labeled ADMSC was done through the sacra media artery using a 21-gauge hypodermic needle.

In parallel, as a positive control for fluorescent cells, a group of animals received a transplant of ADMSC labeled with the cell tracker orange CMTMR (5-(and 6)-(((4-chloromethyl) benzoyl) amino) tetramethyl-rhodamine) (Thermo Fisher Scientific Inc). For this purpose, the pellet containing the cells was suspended in α-Modified Eagle Medium (MEM) (Thermo Fisher Scientific) with the cell tracker and incubated for 45 minutes at 37°C under sterile conditions. Then the probe solution was replaced with fresh medium and the cells were incubated for 30 minutes. Two animals were used for each group of study: CMTMR, NPC, Sham, in total it was six animals.

Seven days post-crush, the animals were perfused as described previously by Usach et al.[22] The presence of NPC- and CMTMR-labeled ADMSC in the control and crushed sciatic nerves was evaluated in cryostat sections using fluorescence microscopy (Axio Vert.A1; Carls Zeiss).

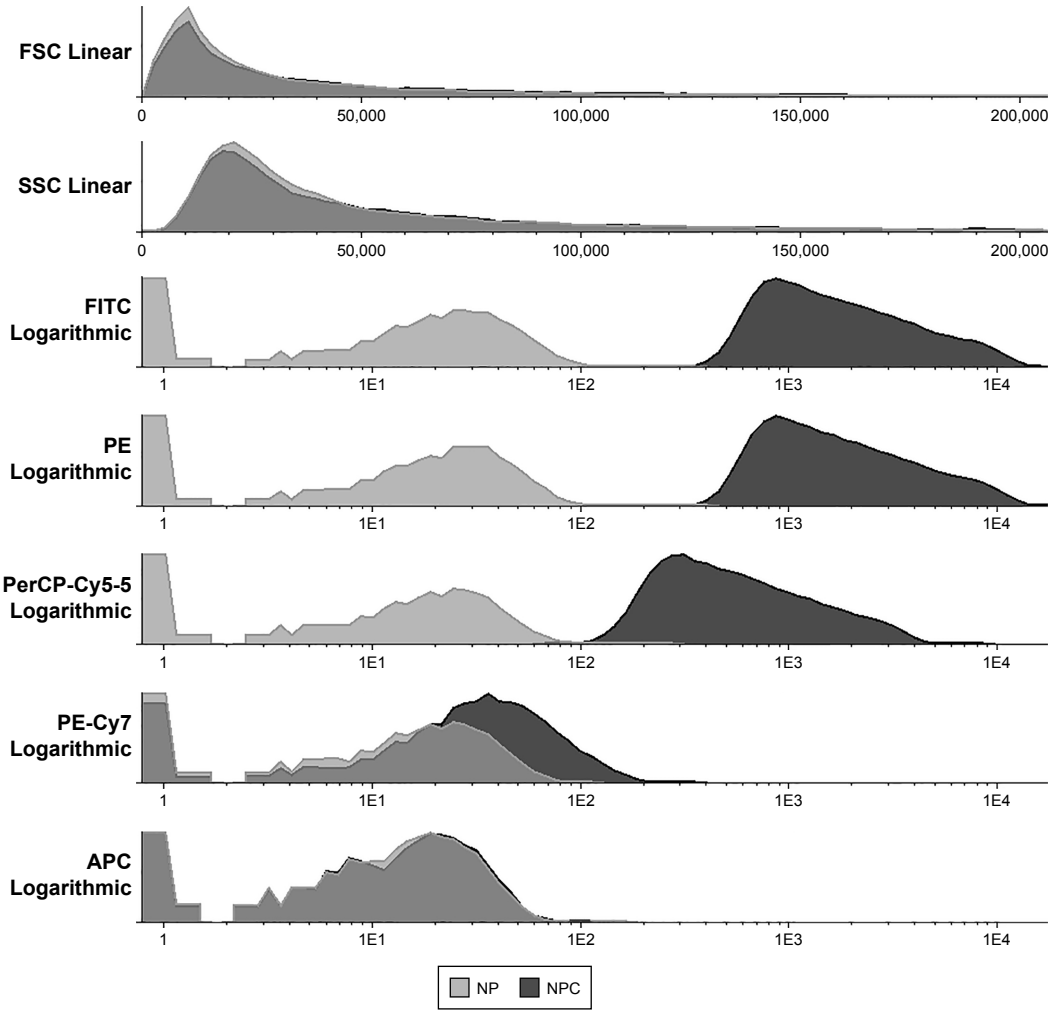

Figure 2 NPC and NP flow cytometry showing the fluorescence of NPC.
Abbreviations: NP, unloaded polycaprolactone nanoparticles; NPC, curcumin-loaded polycaprolactone nanoparticles; PE, phycoerythrin; FITC, fluroscein isothiocyanate.

Results

In vitro studies

Nanoparticles characteristics

The main physicochemical properties of nanoparticle suspensions used in this study are summarized in Table 1. According to DLS measurements, NP and NPC had a mean diameter of 194.9 nm and 189.4 nm, respectively, and monodisperse size distribution (polydispersity index <0.2). Finally, nanoparticles showed a curcumin content of about 426.0 µg/mL and encapsulation efficiency values higher than 99%, demonstrating their suitability in the encapsulation of this compound.

Immunocytochemistry analyses of NPC demonstrated fluorescence emission wavelength for FITC (519 nm), PE (578 nm), and PerCP (678 nm) (Figure 2). FITC and PE have emission wavelength near green fluorescent protein (511 nm), which was used in fluorescence microscopy (Figure 3).

The analysis was done during 24 consecutive days, and the fluorescence detected in Vero cells identified with NPC was the highest in the first 8 days (Figure 3).

Cell cytometric analysis

The cytometric analysis demonstrated that cells from adipose tissue were mesenchymal stems cells evidenced by their immunophenotypic profile based on ISHAGE guidelines[23] (Figure 4).

SEM analysis

SEM analysis demonstrated NPC tendency to cluster and attach to the cell membrane before being internalized (Figure 5). Images of control cells available shown in Figure S3.

Cytotoxicity analysis

Cytotoxicity analysis demonstrated that NPC at a concentration of 30 µM were not significantly toxic to Vero cells (Figure 6).

In vivo studies

In vivo fluorescence identification

Upon performing in vivo analysis by Carestream in vivo MS FX-Pro (Bruker Corporation, Billerica, MA, USA), the fluorescence signal was demonstrated only in the quadrant that received the NPCs without cells (Figure 7).

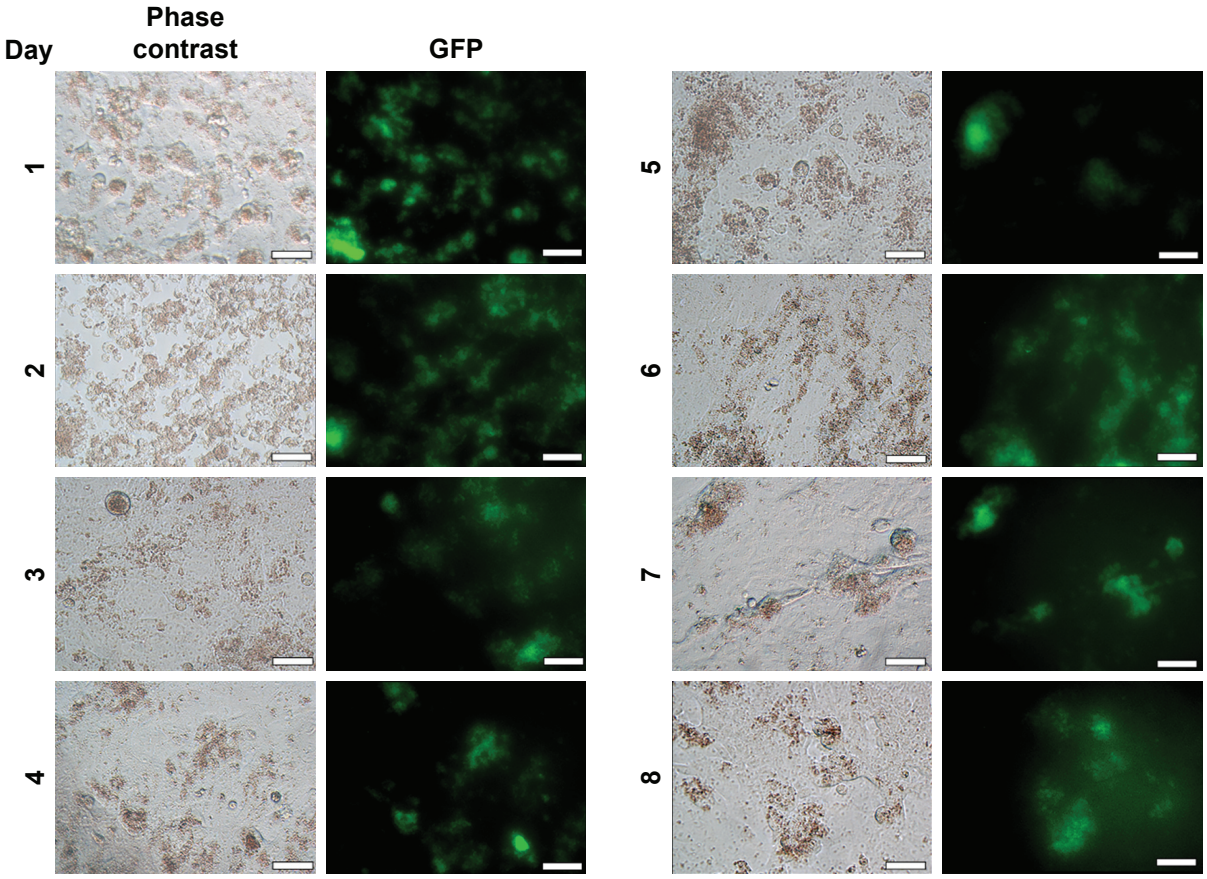

Figure 3 Phase contrast and GFP channel for image captures of Vero cells with NPC during 8 days (400×), in inverted fluorescent optical microscopy (Axio Vert.A1; Carl Zeiss Meditec AG, Jena, Germany); scale bar: 50 µm.
Abbreviations: GFP, green fluorescent protein; NPC, curcumin-loaded polycaprolactone nanoparticles.

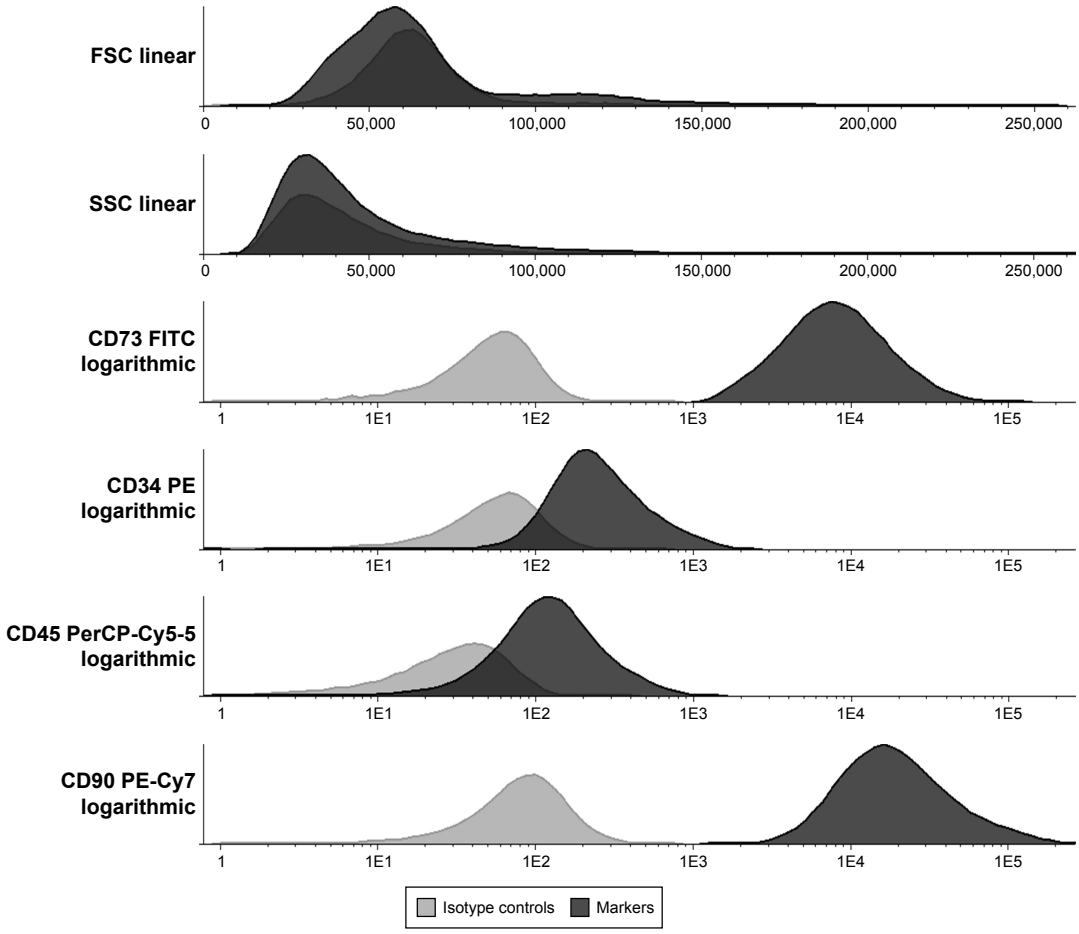

Figure 4 Immunophenotyping of the ADMSC: the cytometry showed that the ADMSC were positive for the protein membrane markers CD73 and CD90 and negative for CD34 and CD45.
Abbreviations: ADMSC, adipose-derived mesenchymal stem cells; PE, phycoerythrin; FITC, fluroscein isothiocyanate.

Myocardial infarction

The myocardial infarction model was made according to the steps described earlier (Figure S1). Infarction area was demonstrated by the change of color of the myocardial tissue after left coronary ligation (Figure S4). NPC-ADMSC transplant was done by epicardial injections 1 week after myocardial infarction (Figure S5). NPC were identified in myocardial tissue 1 week after transplantation (Figure 8). The choice of euthanasia after 1 week was based on fluorescence results in vitro.

Sciatic nerve crush

NPC labeling of ADMSC in the ipsilateral sciatic nerve 7 days post-injury and transplantation (Figure 9) was detected by confocal microscopy.

Discussion

In vitro studies

After DLS measurements of NP and NPC mean diameter and distribution, those values of zeta potential (Table 1) were close to neutral due to the layer of nonionic surfactant poloxamer. With regard to the nanoparticle suspensions used, their high encapsulation efficiency is probably related to the poor water solubility of curcumin in external phase. Flow cytometric analyses of NPC was demonstrated on three fluorescence emission channels with wavelength for FITC (519 nm), PE (578 nm), and PerCP (678 nm), and the fluorescence detection in Vero cells containing NPC in their cytoplasm was the highest in the first 8 days. These were the first steps to establish the study to investigate the fluorescence properties of curcumin-loaded nanoparticles for tracking cellular therapy.

The cell cytometric analysis was confirmed by assessing the phenotype markers CD73+/CD90+/CD45−/CD34; the cells had successful trilineage differentiation (data not shown).[23] We did not use the CD105 cell membrane marker. This limitation, however, did not disturb the main objective of this study, which consists in the identification of the cells posttransplant without a therapeutic aim, and only involves simulation. This study did not analyze the function of myocardial infarction neither the sciatic nerve after transplantation.

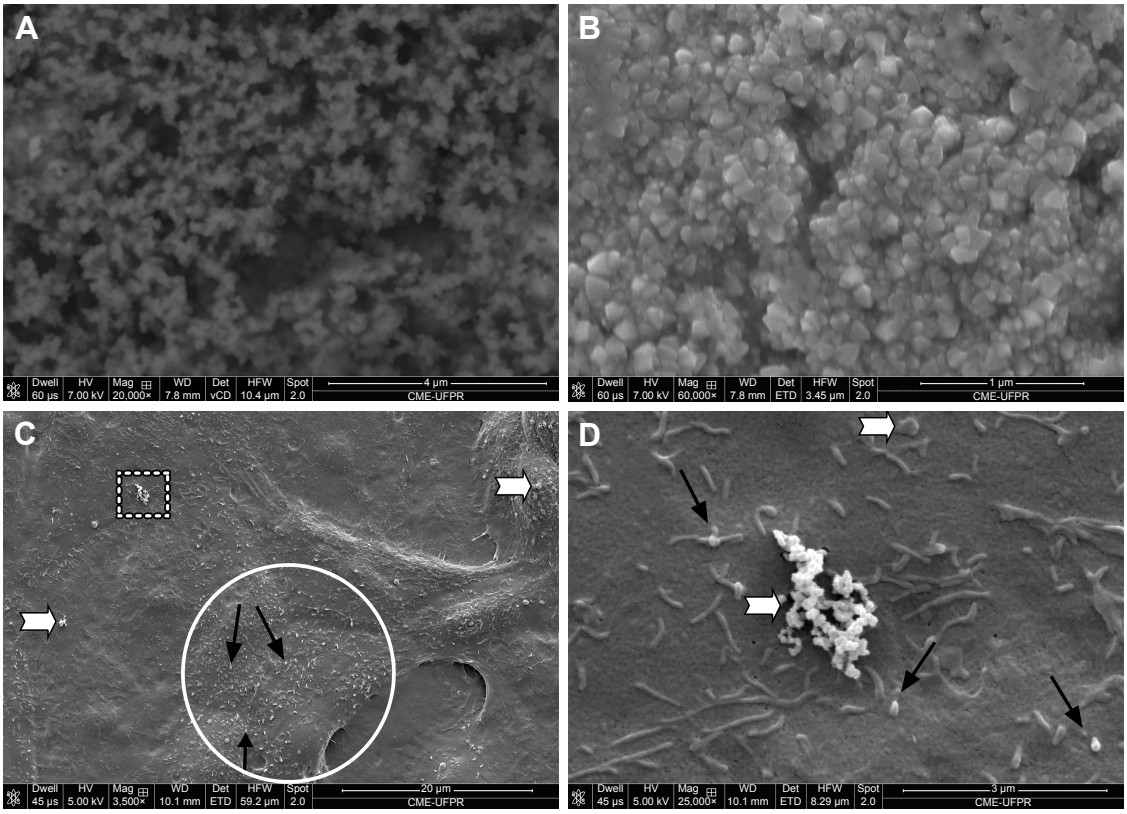

Figure 5 (**A** and **B**) NPC 20,000× and 60,000×, respectively (SEM). (**C** and **D**) NPC on Vero cell membranes, 3,500× and 25,000×, respectively (SEM). White arrows indicate lumps of NPCs and black arrows indicate isolated NPC.
Abbreviations: NPC, curcumin-loaded polycaprolactone nanoparticles; SEM, scanning electron microscopy.

As demonstrated with the SEM images, the NPC was along the cell surface; nevertheless, the mechanisms of their internalization remain unknown, although similar nanoparticles have been found to accumulate in endosomes described by Ucisik et al.[24]

Cytotoxicity analysis

The cytotoxicity analysis finding is certainly advantageous for research using NPC in cell transplantation. Our results are supported by the fact that curcumin is well known for its medical uses and low toxicity even in higher concentrations.[25] In addition, both curcumin and polycaprolactone are biodegradable and appear to be biocompatible with human health.[24,26]

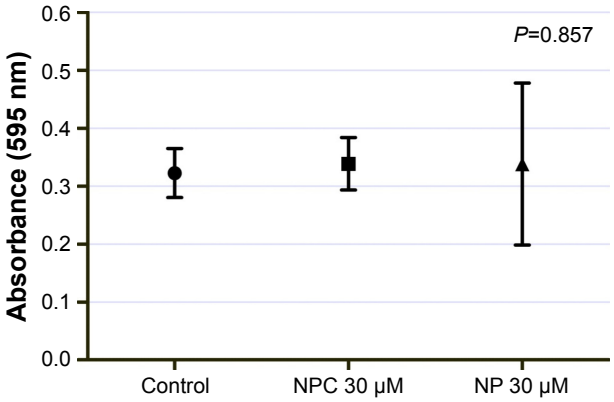

Figure 6 MTT assay showing no significant differences (*P*=0.8575) between the studied groups (one-way ANOVA statistical test).

In vivo studies

The in vivo fluorescence identification suggested that the analysis with the equipment requires higher concentrations of NPCs so that the fluorescence can be detected. The absence of the fluorescence identification at the regions that were injected with NPC-ADMSC can be explained by the fact that the cells cannot store all NPCs that were incubated with them, ie, the amount of NPCs exceeds the maximum uptake ability of the cells.

The myocardial infarction model using transplanted NPC-ADMSC in myocardial tissue was in accordance with earlier studies that revealed decreased number of surviving cells after the first week of transplantation when their effects are mostly paracrine.[27–29] Thus, our strategy is feasible and does not require additional manipulation by survival enhancing strategies.[30]

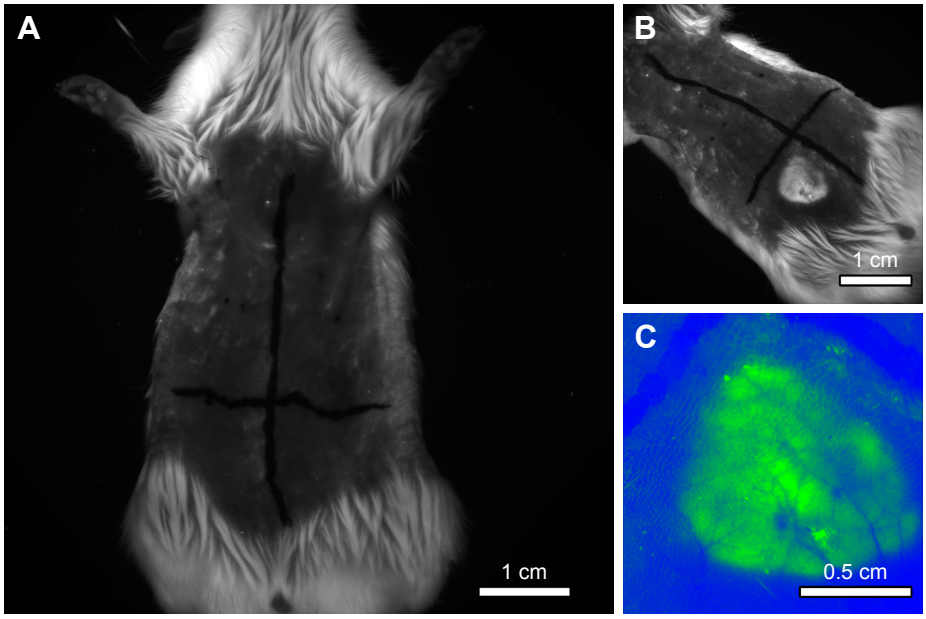

Figure 7 Representative images showing: (**A**) an animal before subcutaneous injections, (**B**) after excitement condition of the regions of interest that received the injections, (**C**) identification of the fluorescent region that received NPC, and colored by software (green color) Carestream in vivo MS FX-Pro (Bruker Corporation, Billerica, MA, USA).
Abbreviation: NPC, curcumin-loaded polycaprolactone nanoparticles.

The sciatic nerve crush model using transplanted NPC-ADMSC was made 7 days post-injury; this survival time was selected because it corresponds to the peak of demyelination and because when transplanted, CMTMR-labeled ADMSC were exclusively recruited in the ipsilateral nerve.[22] The results obtained demonstrate that NPC-labeled ADMSC also migrate exclusively to the demyelinated area of the ipsilateral nerve, ie, distal areas.

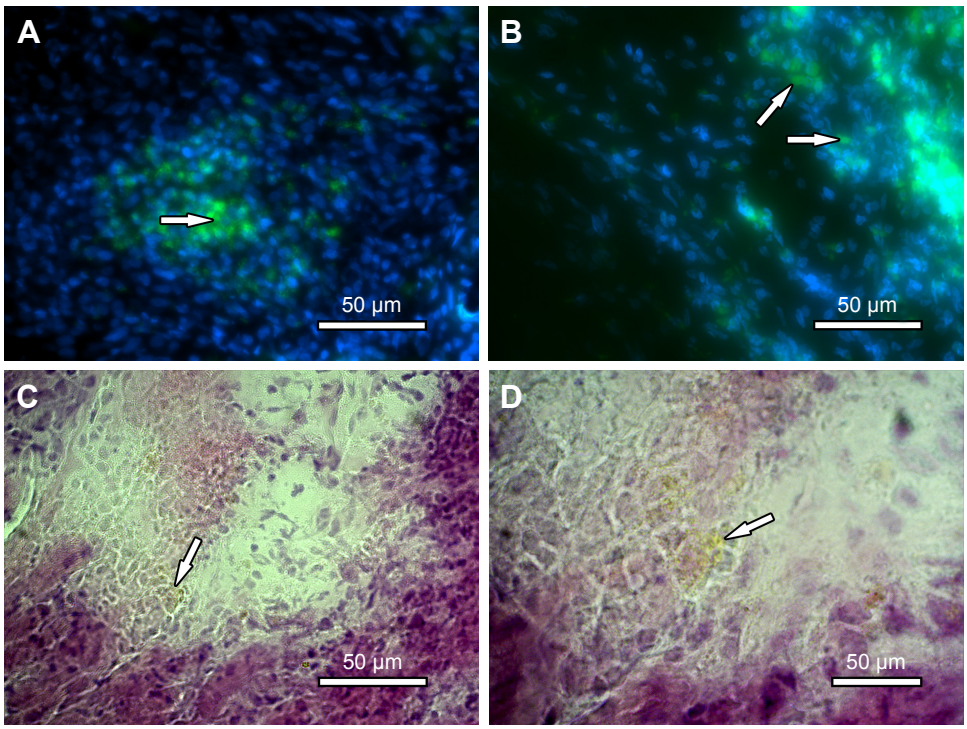

Figure 8 Myocardial tissue after cell therapy.
Notes: (**A** and **B**) Nuclei stained with Hoechst 33,258 (blue) and NPC fluorescence (green), 200× and 400×, respectively (fluorescent optical microscopy). (**C** and **D**) H&E staining of myocardial tissue showing NPC clusters, 400× and 1,000×, respectively, scale bar: 50 µm. The white arrows are the NPC clusters.
Abbreviation: NPC, curcumin-loaded polycaprolactone nanoparticles.

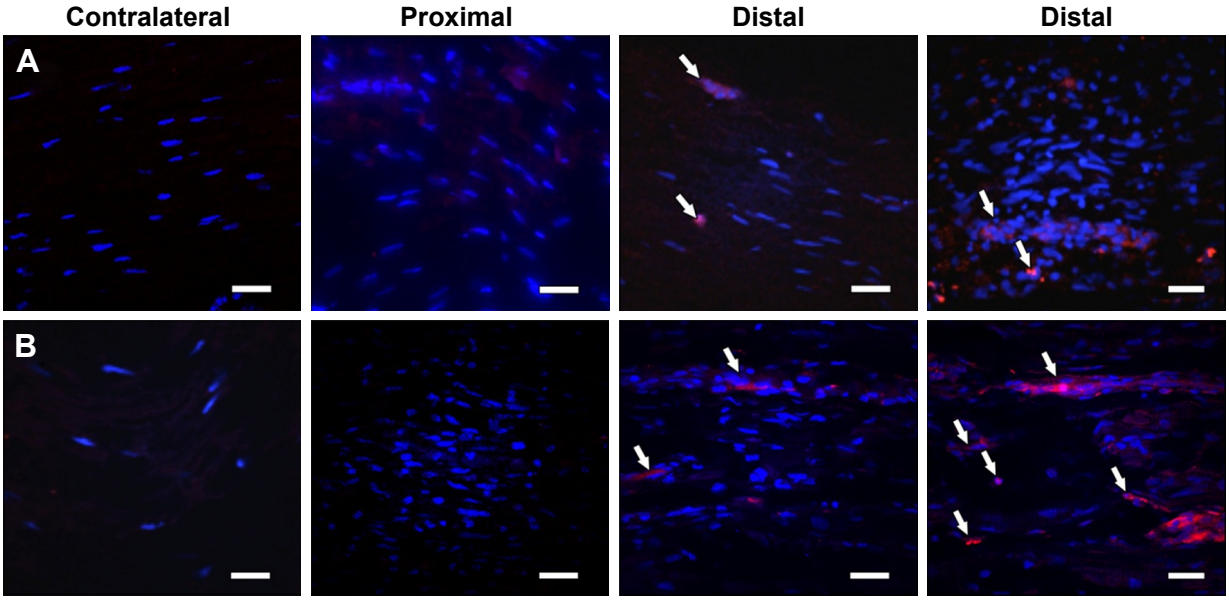

Figure 9 After 7 days posttransplant in the contralateral nerve and the proximal and distal areas of the ipsilateral sciatic nerve. (**A**) Detection of transplanted ADMSC labeled with NPC. (**B**) Detection of ADMSC with cell tracker CMTMR.
Abbreviation: ADMSC, adipose-derived mesenchymal stem cells; NPC, curcumin-loaded polycaprolactone nanoparticles; CMTMR, (5-(and 6)-(((4-chloromethyl) benzoyl) amino) tetramethyl-rhodamine).

Furthermore, it is interesting to emphasize that this was the first study to demonstrate that biopolymer nanoparticles could be used for cell tracking in cell-based therapy, whereas the other authors proposed inorganic nanoparticles.[31,32]

Conclusion

Our in vivo and in vitro studies identified that transplanted NPC cells, by histological/fluorescence analysis, revealed the benefit of their potential use in cell tracking. In addition, it was possible to analyze cell integration by examining various biopsies.

Although further studies may be necessary to improve fluorescence methodology and ensure safety, these findings suggest a promising strategy for using NPC as markers for stem cell tracking and constitute a step forward in cell therapy applications.

Acknowledgment

We would like to thank financial support of Institut Carnot POLYNAT (France), CERMAV (France), Luciana Lopes from Instituto de Tecnologia do Paraná (TECPAR) (Brazil) for the Vero cell line supply, and Coordenação de Aperfeiçoamento de Pessoal de Nível Superior (CAPES) (Brazil).

Disclosure

The authors report no conflicts of interest in this work.

References

1. Mason C, Dunnill P. A brief definition of regenerative medicine. *Regen Med*. 2008;3(1):1–5.
2. Srinivas M, Aarntzen EH, Bulte JW, et al. Imaging of cellular therapies. *Adv Drug Deliv Rev*. 2010;62(11):1080–1093.
3. Betzer O, Meir R, Dreifuss T, et al. In-vitro optimization of nanoparticle-cell labeling protocols for in-vivo cell tracking applications. *Sci Rep*. 2015;5:1–11.
4. Onoshima D, Yukawa H, Baba Y. Multifunctional quantum dots-based cancer diagnostics and stem cell therapeutics for regenerative medicine. *Adv Drug Deliv Rev*. 2015;95:2–14.
5. Liu K, Deslippe J, Xiao F, et al. An atlas of carbon nanotube optical transitions. *Nat Nanotechnol*. 2012;7(5):325–329.
6. Sampogna G, Guraya SY, Forgione A. Regenerative medicine: historical roots and potential strategies in modern medicine. *J Microsc Ultrastruct*. 2015;3(3):101–107.
7. Xu C, Miranda-Nieves D, Ankrum JA, et al. Tracking mesenchymal stem cells with iron oxide nanoparticle loaded poly(lactide-co-glycolide) microparticles. *Nano Lett*. 2012;12(8):4131–4139.
8. Yeo D, Wiraja C, Chuah YJ, Gao Y, Xu C. A nanoparticle-based sensor platform for cell tracking and status/function assessment. *Sci Rep*. 2015;5:14768.
9. Mondal S, Ghosh S. Role of curcumin on the determination of the critical micellar concentration by absorbance, fluorescence and fluorescence anisotropy techniques. *J Photochem Photobiol B*. 2012;115:9–15.
10. Kunwar A, Barik A, Mishra B, Rathinasamy K, Pandey R, Priyadarsini KI. Quantitative cellular uptake, localization and cytotoxicity of curcumin in normal and tumor cells. *Biochim Biophys Acta*. 2008;1780(4):673–679.
11. Priyadarshini K. Photophysics, photochemistry and photobiology of curcumin: studies from organic solutions, bio-mimetics and living cells. *J Photochem Photobiol C Photochem Rev*. 2009;10(2):81–95.
12. Xie M, Fan D, Zhao Z, et al. Nano-curcumin prepared via supercritical: Improved anti-bacterial, anti-oxidant and anti-cancer efficacy. *Int J Pharm*. 2015;496(2):732–740.

13. Weber WM, Hunsaker LA, Abcouwer SF, Deck LM, vander Jagt DL. Anti-oxidant activities of curcumin and related enones. *Bioorg Med Chem*. 2005;13(11):3811–3820.
14. Takahashi K, Tanabe K, Ohnuki M, et al. Induction of pluripotent stem cells from adult human fibroblasts by defined factors. *Cell*. 2007; 131(5):861–872.
15. Mathiasen AB, Haack-Sørensen M, Kastrup J. Mesenchymal stromal cells for cardiovascular repair: current status and future challenges. *Future Cardiol*. 2009;5(6):605–617.
16. Cremers NA, Lundvig DM, van Dalen SC, et al. Curcumin-induced heme oxygenase-1 expression prevents H2O2-induced cell death in wild type and heme oxygenase-2 knockout adipose-derived mesenchymal stem cells. *Int J Mol Sci*. 2014;15(10):17974–17999.
17. Liu J, Zhu P, Song P, et al. Pretreatment of adipose derived stem cells with curcumin facilitates myocardial recovery via antiapoptosis and angiogenesis. *Stem Cells Int*. 2015;2015:638153.
18. Zhang Z, Li S, Cui M, et al. Rosuvastatin enhances the therapeutic efficacy of adipose-derived mesenchymal stem cells for myocardial infarction via PI3K/Akt and MEK/ERK pathways. *Basic Res Cardiol*. 2013;108(2):333.
19. Mazzarino L, Travelet C, Ortega-Murillo S, et al. Elaboration of chitosan-coated nanoparticles loaded with curcumin for mucoadhesive applications. *J Colloid Interface Sci*. 2012;370(1):58–66.
20. Mazzarino L, Otsuka I, Halila S, et al. Xyloglucan-block-poly(ϵ-caprolactone) copolymer nanoparticles coated with chitosan as biocompatible mucoadhesive drug delivery system. *Macromol Biosci*. 2014; 14(5):709–719.
21. Kilkenny C, Browne W, Cuthill I, Emerson M, Altman D. Improving bioscience research reporting: the arrive guidelines for reporting animal research. *Animals*. 2013;4(1):35–44.
22. Usach V, Goitia B, Lavalle L, Martinez Vivot R, Setton-Avruj P. Bone marrow mononuclear cells migrate to the demyelinated sciatic nerve and transdifferentiate into Schwann cells after nerve injury: attempt at a peripheral nervous system intrinsic repair mechanism. *J Neurosci Res*. 2011;89(8):1203–1217.
23. Sutherland DR, Anderson L, Keeney M, Nayar R, Chin-Yee I. The ISHAGE guidelines for CD34+ cell determination by flow cytometry. International Society of Hematotherapy and Graft Engineering. *J Hematother*. 1996;5(3):213–226.
24. Ucisik MH, Küpcü S, Schuster B, Sleytr UB. Characterization of CurcuEmulsomes: nanoformulation for enhanced solubility and delivery of curcumin. *J Nanobiotechnology*. 2013;11:37.
25. Strimpakos AS, Sharma RA. Curcumin: preventive and therapeutic properties in laboratory studies and clinical trials. *Antioxid Redox Signal*. 2008;10(3):511–546.
26. Mazzarino L, Loch-Neckel G, Bubniak LS, et al. Curcumin-loaded chitosan-coated nanoparticles as a new approach for the local treatment of oral cavity cancer. *J Nanosci Nanotechnol*. 2015;15(1):781–791.
27. Matsuo T, Masumoto H, Tajima S, et al. Efficient long-term survival of cell grafts after myocardial infarction with thick viable cardiac tissue entirely from pluripotent stem cells. *Sci Rep*. 2015;5:16842.
28. van der Bogt KE, Sheikh AY, Schrepfer S, et al. Comparison of different adult stem cell types for treatment of myocardial ischemia. *Circulation*. 2008;118(14 Suppl):S121–S129.
29. Müller-Ehmsen J, Krausgrill B, Burst V, et al. Effective engraftment but poor mid-term persistence of mononuclear and mesenchymal bone marrow cells in acute and chronic rat myocardial infarction. *J Mol Cell Cardiol*. 2006;41(5):876–884.
30. Abdelwahid E, Kalvelyte A, Stulpinas A, de Carvalho KA, Guarita-Souza LC, Foldes G. Stem cell death and survival in heart regeneration and repair. *Apoptosis*. 2016;21(3):252–268.
31. Jasmin de Souza GT, Louzada RA, Rosado-de-Castro PH, Mendez-Otero R, Campos de Carvalho AC. Tracking stem cells with superparamagnetic iron oxide nanoparticles: perspectives and considerations. *Int J Nanomedicine*. 2017;12(12):779–793.
32. Wang J, Xiang B, Deng JX, et al. Hypoxia enhances the therapeutic potential of superparamagnetic iron oxide-labeled adipose-derived stem cells for myocardial infarction. *J Huazhong Univ Sci Technolog Med Sci*. 2017;37(4):516–522.

Supplementary materials

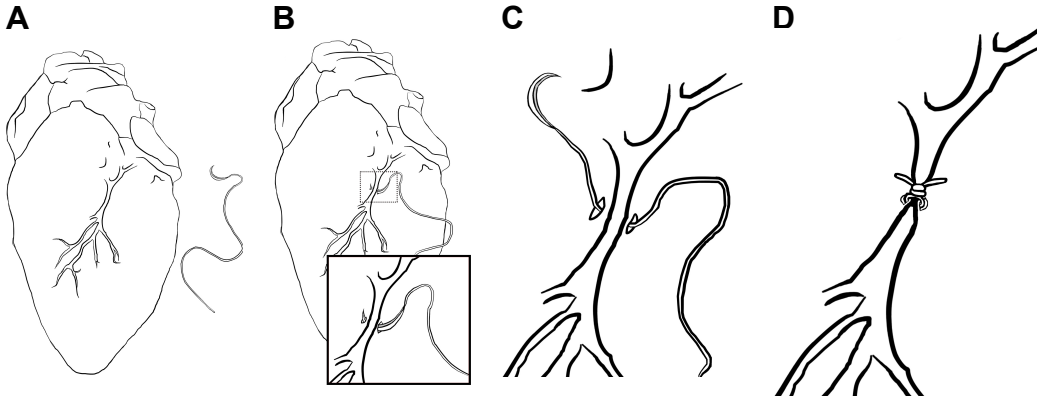

Figure S1 Illustration showing localization of the left coronary artery (**A**) and the steps of ligation of the left coronary artery (**B**–**D**).

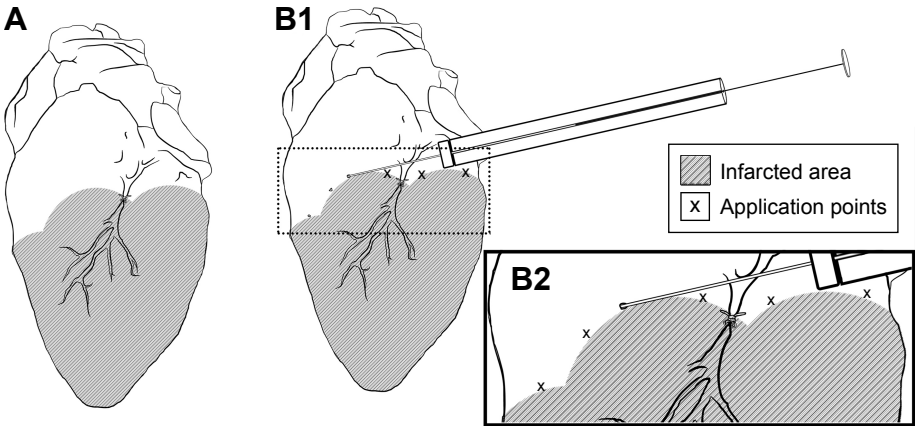

Figure S2 (**A**) Ischemic area resulting from left coronary ligation. (**B1**) and (**B2**) (blow-up), respectively: transplantation of NPC-ADMSC in the peri-infarcted area of the left ventricular wall.
Abbreviations: NPC, curcumin-loaded polycaprolactone nanoparticles; ADMSC, adipose-derived mesenchymal stem cells.

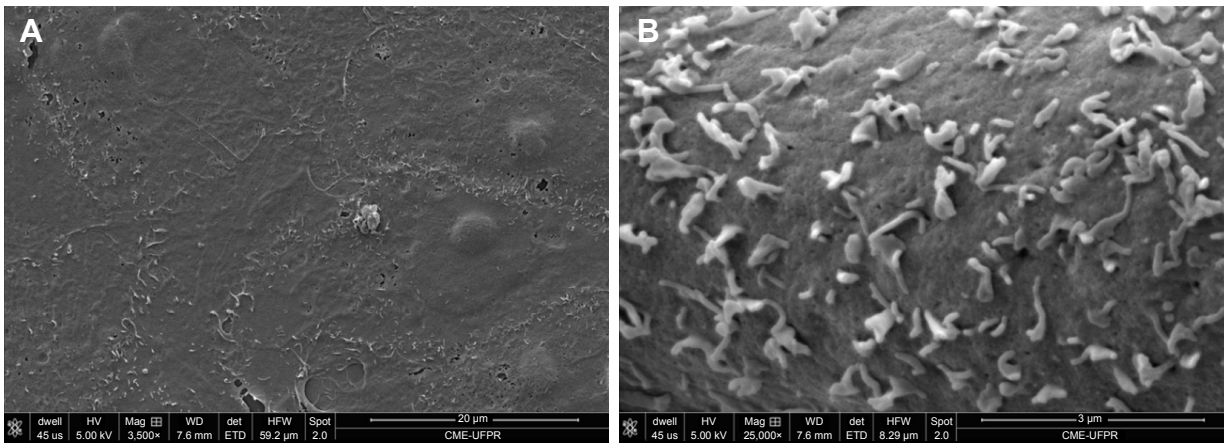

Figure S3 (**A** and **B**) Control Vero cells at 3,500× and 25,000×, respectively (SEM).
Abbreviation: SEM, scanning electron microscopy.

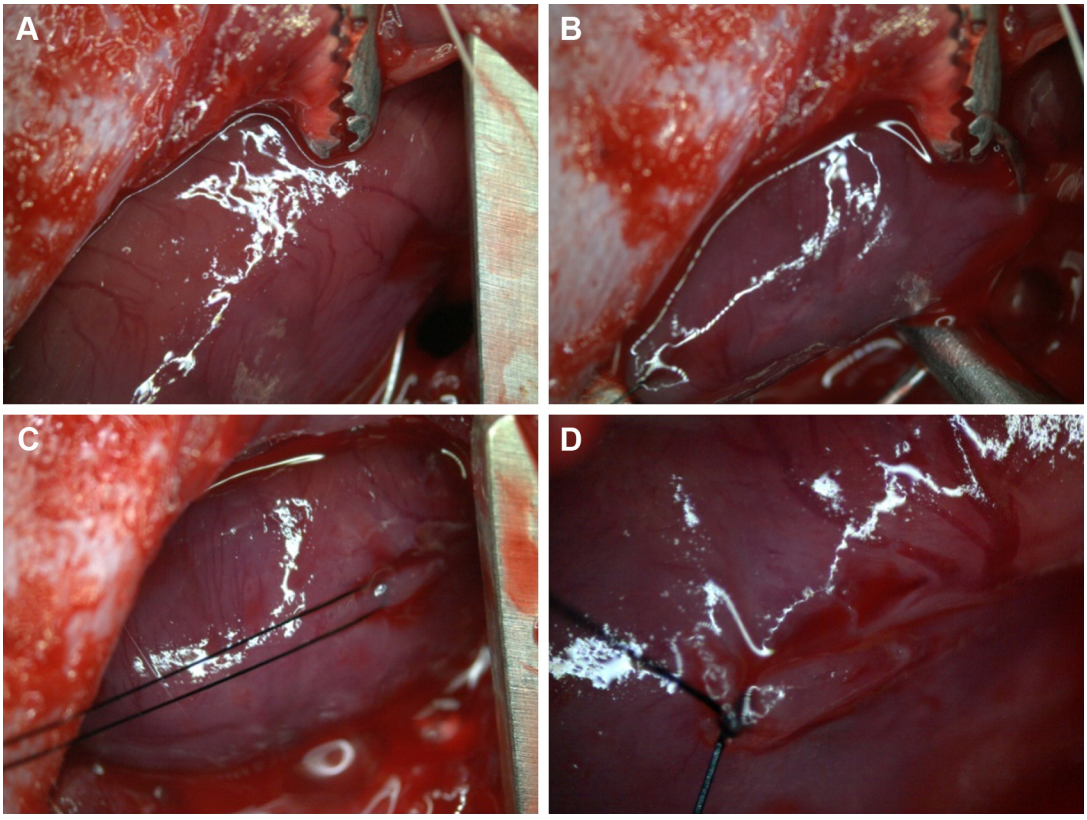

Figure S4 (**A**) Heart exposition of the coronary artery. (**B**–**D**) Ligation of the left coronary artery.

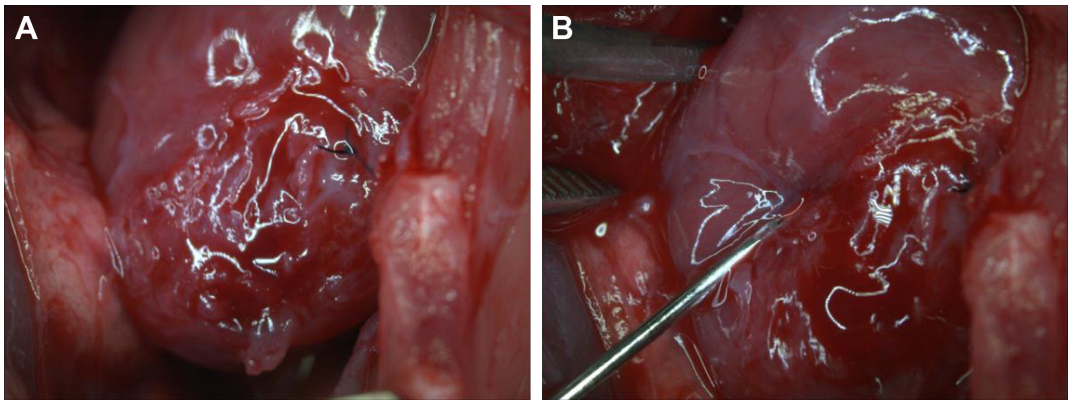

Figure S5 (**A**) Infarcted area after the ligation. (**B**) Transplantation of the NPC-ADMSC in the peri-infarcted area of the left ventricular wall.
Abbreviations: NPC, curcumin-loaded polycaprolactone nanoparticles; ADMSC, adipose-derived mesenchymal stem cells.